Electronic Supplementary Material (ESI) for Materials Horizons.

Supporting Information
For

Gallium Chiral NanoShaping for Circular Polarization Handling

Massimo Cuscunà[1], Mariachiara Manoccio[1,2], Marco Esposito[1],* Mario Scuderi[3], Giuseppe Nicotra[3], Iolena Tarantini[2], Angelo Melcarne[2], Vittorianna Tasco[1],* Maria Losurdo[4] and Adriana Passaseo[1]

1. CNR NANOTEC Institute of Nanotechnology, Via Monteroni, Lecce 73100, Italy
2. University of Salento, Department of Mathematics and Physics Ennio De Giorgi, Via Arnesano, Lecce 73100, Italy
3. CNR IMM Institute for Microelectronics and Microsystems, Strada VIII, Catania 95121, Italy
4. CNR NANOTEC Institute of Nanotechnology, Via Amendola, 122/D, Bari 70126, Italy

E-mail: marco.esposito@nanotec.cnr.it

E-mail: vittorianna.tasco@nanotec.cnr.it

Compositional Analysis of SiO_2-based Helical System Produced by FIBID Approach

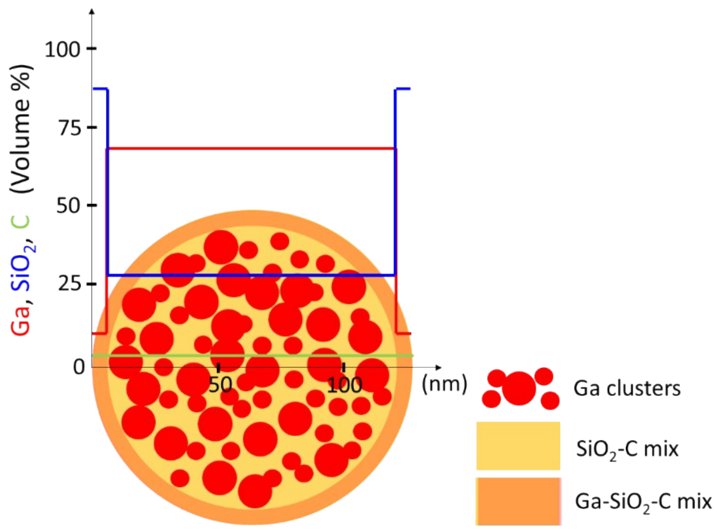

Figure S1. Schematic view of the wire cross section and related Ga, SiO_2, C volume composition profiles.

Effect of Ga^+-Ion Dose in 3D Structure Growth

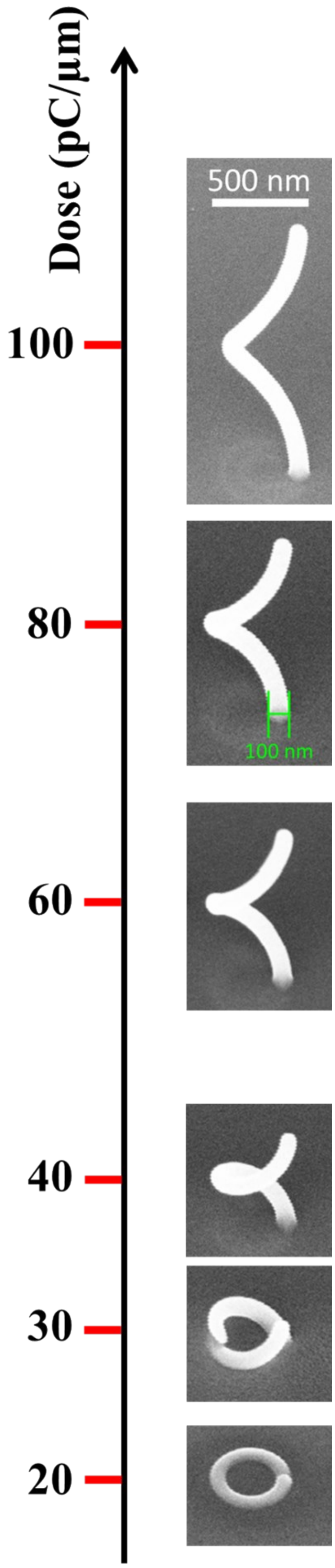

Figure S2. SEM images showing the effect of ion dose variation during the growth of carbon-based nanohelices.

Figure S2 shows the effect of ion dose deviation (ion energy set at 30 KeV) from the optimal value on the helix morphology. It is worth noting that small dose variations can lead to dramatic effect on

3D nanohelix growth. Actually, with lower ion doses (20-30 pC/µm) low quality helices with limited vertical evolution are formed. A Ga^+-ion dose of 40 pC/µm provides a VP of about 500 nm leading C-based nanohelices working in the desired visible spectral range. Conversely, by slightly increasing the ion dose up to 60 pC/µm, a VP increase (800 nm) shifts the chiroptical range of operation of the system to the NIR as also demonstrated in [1].

Optical Constant Calculation of Ga-based Nanocomposites

Considering the given nanocomposite structures, related material dispersions should be carefully analyzed on a numerical basis in order to be exploited for nanophotonic applications. To this purpose we used FDTD simulations and we evaluated effective refractive indexes (n) and absorption coefficients (k) taking into account the helix structure and chemical composition as assessed by TEM/EDX analysis. At first, a customized electromagnetic (EM) model was defined in order to carefully rebuild the material pattern of the core and the shell; being the Maxwell–Garnett approach not sufficiently accurate to evaluate a random mixture made of more than two material components.[2] TEM images have shown that the core is composed by large clusters of tiny Ga clusters (spheroids) embedded into C (Figure 1d) or SiO_2/C (Figure S1) host matrix. The cluster distribution (almost homogenous) was replicated with a full-numerical modelling. The large average diameter of the spheroids (in the range of 9-12 nm) supports the assumption of canonical material dispersions.[3] Hence, we considered a large FDTD box (40x40x100 nm) with a random arrangement of Ga spheroids covering about 66% (Carbon-based helices) and 68% (SiO_2-based helices) of the total volume (Figure S2). This box was illuminated by a plane wave with normal incidence. A monitor collects the complex values of reflected field for the wavelengths of interest (450-850 nm). By considering the optical properties of SiO_2,[4] Ga[5] and amorphous carbon,[6] we calculated the complex reflection coefficients (r) of the overall box, and we finally retrieved the required complex refractive index by the following formula:[7]

$$n(\lambda) = \frac{1 - r(\lambda)}{1 + r(\lambda)}.$$

Analogously, the procedure was also performed for the two shells, of C (Figure 1d) and SiO_2 (Figure S1), respectively. All the calculated optical constants (n, k) for both architectures are shown in Figure S3.

The simulation underlines the metallic behavior of the gallium core, similar in the two systems, as evidenced by the trend of the optical constants (k>n) in the VIS spectral range. Conversely, the two shells exhibit a dielectric behavior, with k<n (and close to zero for SiO_2-based shell) throughout the entire visible region. However, as assessed from TEM investigation, the shell size for C and SiO_2-based helical systems are far from each other, leading to different optical features at the nanoscale of the overall core-shell architectures.

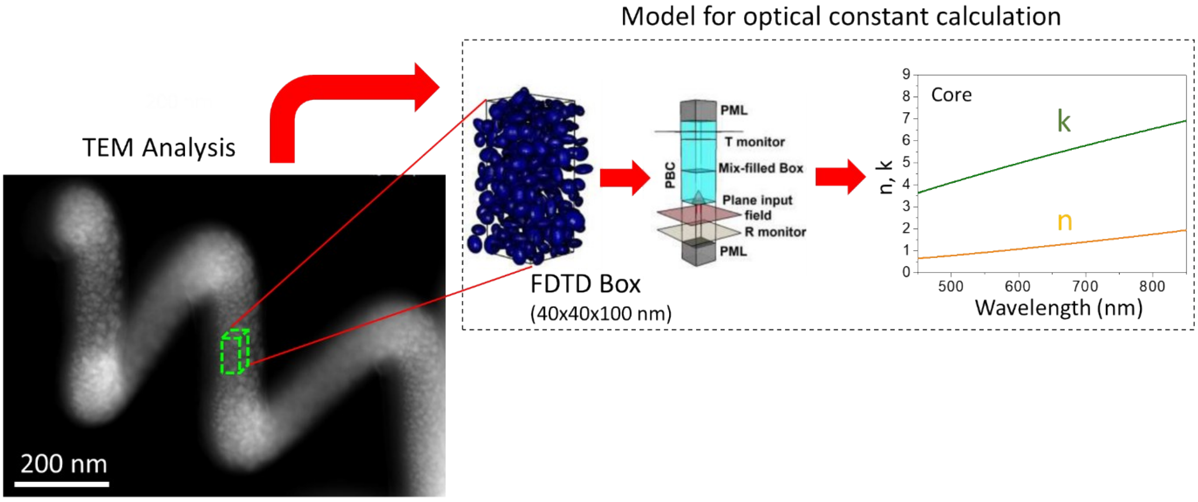

Figure S3. STEM survey image of SiO_2-based nanohelix (left panel). Schematic view of the FDTD system used to evaluate the optical constants of the Ga-rich nanocomposite core. A linearly polarized plane wave vertically directed toward the top impinges the box filled with the Ga/SiO_2/C mixture (right panel). An example of mixture is displayed with a 40x40x100 nm box filled by the Ga inclusions, and whose background index is set to the mixed SiO_2/C host matrix. The Ga spheroids in the picture feature an average diameter of 12 nm, and they randomly cover 68% of the total volume; real (orange solid line) and imaginary (green solid line) part of the complex refractive index for the Ga 68% - SiO_2 28% - C 4% (in volume) compound (right panel).

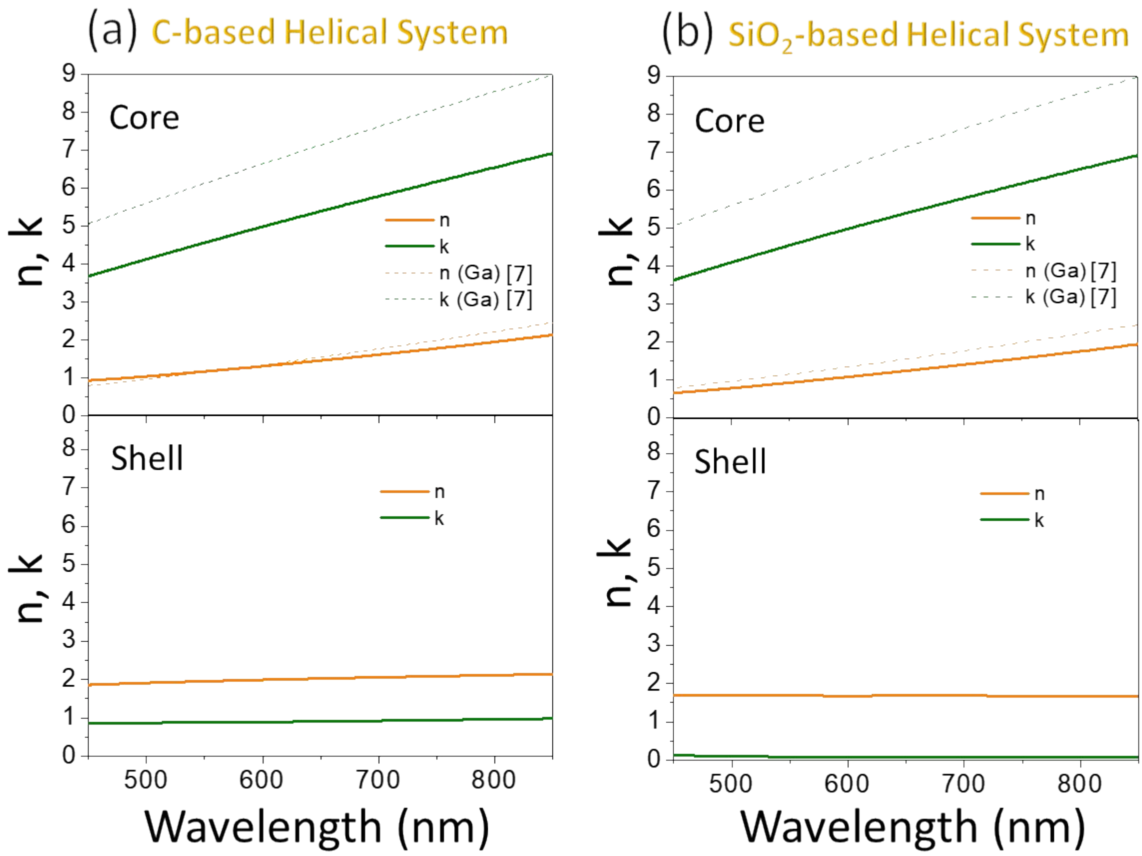

Figure S4. Real (n, orange solid line) and imaginary (k, green solid line) part of the complex refractive index for core and shell nanocomposites in (a) C- and (b) SiO_2-based helical systems. The optical constants of Gallium[5,8] were also reported for comparison (dashed lines).

Compositional Analysis and Optical Properties of SiO_2-based Helix Arrays Produced by FEBID Approach

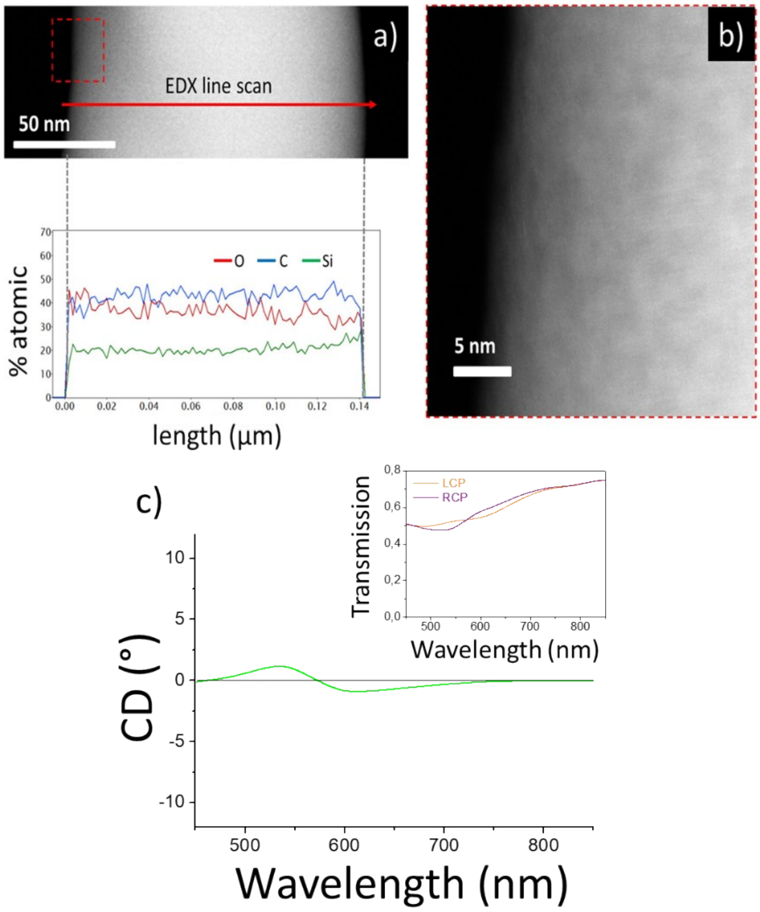

Figure S5. (a) STEM image of a helix section (top panel) and relative elemental atomic percentage along the region indicated by the red arrow (bottom panel). (b) High magnification image of the helix edge indicated in panel a). (c) CD expressed in degree units of FEBID array composed by helical nanowire structures (1 loop). The inset reports transmission spectra under normal incidence of right (T_{RCP})- and left (T_{LCP})-handed circularly polarized light.

Optical Properties of Helix Arrays with Pitch Number N as 0.25, 0.5 and 1

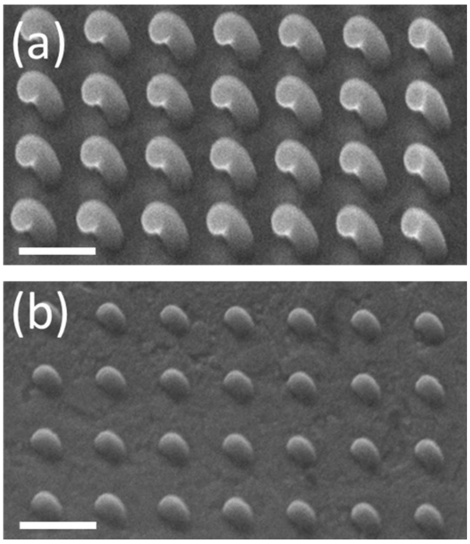

Figure S6. Vertical stacking of chiral dipoles in SiO_2-based chiral systems. SEM images of 3D helical nanosystem arrays with (a) N=0.5 and (b) N=0.25. Scale bars: 500 nm.

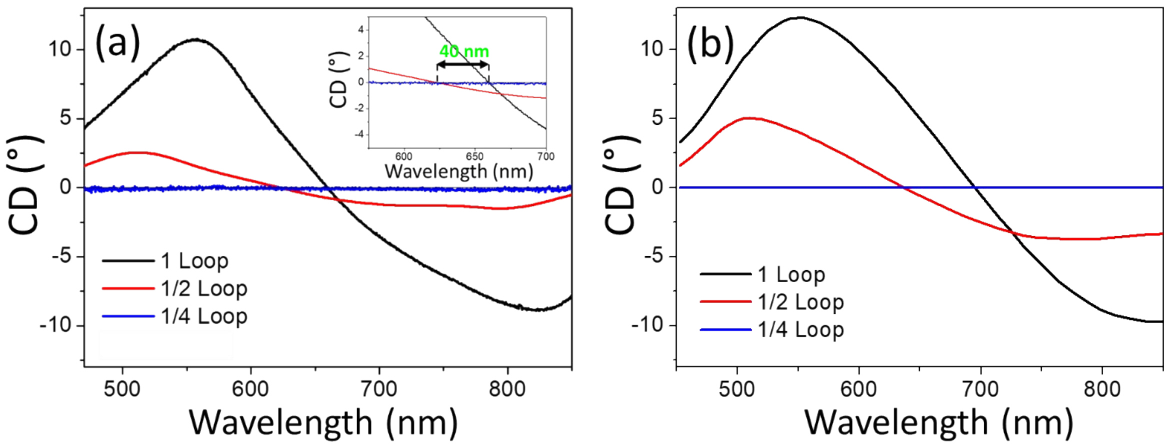

Figure S7. (a) Experimentally measured CD, expressed in degree units, induced by the stacking of chiral dipoles (pitch number N as 0.25, 0.5 and 1) along the normal to the substrate in the SiO_2-based helix array. Hybridization of plasmonic modes is highlighted by the bandwidth increase. The inset better emphasizes the spectral region near the zero circular dichroism reporting an enlargement of about 40 nm for 1 loop helix array dichroic band with respect to the half-pitch helices. (b) Simulated CD curves for SiO_2-based nanohelix arrays as the structure height increases from 0.25 to 1 pitches.

References

(1) Esposito, M.; Tasco, V.; Cuscunà, M.; Todisco, F.; Benedetti, A.; Tarantini, I.; Giorgi, M. D.; Sanvitto, D.; Passaseo, A. Nanoscale 3D Chiral Plasmonic Helices with Circular Dichroism at Visible Frequencies. *ACS Photonics* **2015**, *2* (1), 105–114. https://doi.org/10.1021/ph500318p.

(2) Zhao, X.; Wu, Y.; Fan, Z.; Li, F. Three-Dimensional Simulations of the Complex Dielectric Properties of Random Composites by Finite Element Method. *J. Appl. Phys.* **2004**, *95* (12), 8110–8117. https://doi.org/10.1063/1.1712017.

(3) Salski, B. The Extension of the Maxwell Garnett Mixing Rule for Dielectric Composites with Nonuniform Orientation of Ellipsoidal Inclusions. *Prog. Electromagn. Res.* **2012**, *30*, 173–184. https://doi.org/10.2528/PIERL12020202.

(4) Malitson, I. H. Interspecimen Comparison of the Refractive Index of Fused Silica*,†. *JOSA* **1965**, *55* (10), 1205–1209. https://doi.org/10.1364/JOSA.55.001205.

(5) Knight, M. W.; Coenen, T.; Yang, Y.; Brenny, B. J. M.; Losurdo, M.; Brown, A. S.; Everitt, H. O.; Polman, A. Gallium Plasmonics: Deep Subwavelength Spectroscopic Imaging of Single and Interacting Gallium Nanoparticles. *ACS Nano* **2015**, *9* (2), 2049–2060. https://doi.org/10.1021/nn5072254.

(6) Hagemann, H.-J.; Gudat, W.; Kunz, C. Optical Constants from the Far Infrared to the X-Ray Region: Mg, Al, Cu, Ag, Au, Bi, C, and Al_2O_3. *JOSA* **1975**, *65* (6), 742–744. https://doi.org/10.1364/JOSA.65.000742.

(7) Maier, S. A. *Plasmonics: Fundamentals and Applications*; Springer US, 2007.

(8) McMahon, J. M.; Schatz, G. C.; Gray, S. K. Plasmonics in the Ultraviolet with the Poor Metals Al, Ga, In, Sn, Tl, Pb, and Bi. *Phys. Chem. Chem. Phys.* **2013**, *15* (15), 5415–5423. https://doi.org/10.1039/C3CP43856B.